PROCEEDINGS PAPER

Best references for the QPA of Portland cement

T. G. Fawcett [1,a] J. R. Blanton,[1] S. N. Kabekkodu,[1] T. N. Blanton [1] J. Lyza,[2] and D. Broton[3]
[1]*International Centre for Diffraction Data, Newton Square, PA, USA*
[2]*Levy Technical Laboratories, Edward C. Levy Co., Portage, IN, USA*
[3]*CTL Group, Skokie, IL, USA*

(Received 27 April 2022; accepted 18 May 2022)

Cement references were reviewed and whole pattern methods were developed for the quantitative phase analysis (QPA) of Type I Portland Cements. A set of control references were established for phase identification and quantitative analysis using laboratory diffractometers. Both RIR and Rietveld whole pattern fitting methods were used in the analyses. A block refined, parameter restricted, Rietveld method produced the best QPA results by comparison with known mixtures. Similar to prior literature findings, care has to be taken because of the severe peak overlap of the major calcium silicate and calcium aluminate phases in Portland cement and the complexity of the chemistry and structures involved. Two of the four major phases identified are doped supercells and the major C3S phase is also disordered. © *The Author(s), 2022. Published by Cambridge University Press on behalf of International Centre for Diffraction Data.*
[doi:10.1017/S0885715622000215]

I. INTRODUCTION

As currently practiced, the quantitative phase analysis of cements by the Rietveld method requires a crystal structure or powder pattern as input into the refinement. The RIR whole pattern method requires a powder pattern for each phase for input. The powder pattern can come from an experiment or be calculated from a single-crystal structure. In either method, these inputs, that we will generically refer to as references, are used as models for comparison with the experimental data. These references can come directly from a publication or a wide number of commercial databases.

The quantitative phase analyses (QPA) of Type I Portland cement are complex. Type I cements typically consist of 12 phases, 4 account for the bulk composition and the other 8 phases are in concentrations of 1–4% (Walenta and Füllmann, 2004). In addition, there are a host of additives that can be blended into commercial cement products to impart desirable properties (i.e., high strength, quick setting, use in water), sometimes creating other cement types. Furthermore, two of the bulk composition phases, C3A and C3S (cement chemist notation), are frequently present as supercells with $Z = 24$ and $Z = 36$, respectively. The supercells are created by cation doping, most commonly Mg, for Ca in the structure. The disruption of the lattice lowers the scattering factors, so the use of supercell models are required for an accurate QPA (De la Torre *et al.*, 2002). Several authors have determined that the major phases of cement and cement clicker, particularly the C3S phase, are polymorphic mixtures (Nicola *et al.*, 2001; Peterson *et al.*, 2006).

A difficulty of QPA by Rietveld analysis is the large number of potential variables that can be refined using 12 structures, multiple supercells, polymorphs, and variable doping at atomic sites. As mentioned (Peterson *et al.*, 2006), "The inclusion of additional phases into the Rietveld model increases the number of parameters being modeled, even when it is debatable that there is sufficient information in the data to identify the phases. This will result in a statistically better fit of the model, although the QPA results may be unrealistic". Finally, the growth of the worldwide cement market has resulted in a corresponding growth in publications and new structural determinations, hundreds of which were published after standard methods were developed.

The ICDD in collaboration with industry scientists has reviewed published references in the ICDD databases (Gates-Rector and Blanton, 2019; Releases 2021) in concert with the QPA of commercial cement samples and standard reference materials. The objective of the research is to identify which references are common vs. exotic, and which references are best for QPA using routine methods available in the laboratory. The goal is to develop a control set of references that can be applied by non-experts in the analysis of cements using a conventional laboratory powder diffraction equipment.

II. EXPERIMENTAL

A. Samples

Cements are derived from natural geological deposits of mostly limestone (80%) and clay but can also have industrial by-products as well as coal and waste fuel for firing the kiln. The kiln typically operates around 1400 °C and produces a cement "clinker" that consists of various calcium aluminates and calcium silicates that are the primary components of Portland cement. The Merriam-Webster online dictionary (Webster, 2021) defines Portland cement as "a hydraulic cement made by finely pulverizing the clinker produced by calcining to incipient fusion a mixture of clay and limestone or similar materials". The authors teamed for a collaborative effort between the International Centre for Diffraction Data (ICDD), a publisher of a database of materials, combined with the CTL group, a provider of services to the cement

[a]Author to whom correspondence should be addressed. Electronic mail: dxcfawcett@outlook.com

 0885-7156/2022/37(2)/68/8/$18.00

industry, and Edward C. Levy, a manufacturer of cement products.

The CTL group kindly provided high purity specimens of common Portland cement phases as well as a known mixture of the major four phases of Portland cement. These were synthesized at CTL and characterized by both XRD and XRF. Edward C. Levy provided raw data from 22 samples of various mixtures produced in their cement clinker and steel slag operations. To compliment these industrial samples, the ICDD purchased two NIST-SRM certified Portland cement clinkers, SRM 2687a and SRM 2688 (Stutzman *et al.*, 2008; Stutzman and Heckert, 2019) that contained certified amounts of the four major phases. The ICDD also used a heavily characterized sample of Portland cement that matched a published quantitative phase analysis (Walenta and Füllmann, 2004). To examine various additives in Portland cement formulations, ICDD purchased and analyzed five commercial samples manufactured by Quickcrete, BASF, and Custom. These products were analyzed as received flowable powders, and after addition of water and setting of the cement. The additives were compared with listings compiled and published by ASTM in test method C-1365-18 (ASTM, 2018) and the National Highway Research Board in Special Report 127 (HRB, 1972).

B. Data collection

X-ray powder diffraction data were collected on three different laboratory diffractometers and at three different locations. The data shown in the figures were collected at the ICDD. Data collected at Edward C. Levy and Penn. State University focused on slags and clinkers and were used primarily to study additives.

At the ICDD, data were collected on a Bruker D-2 benchtop diffractometer equipped with a LYNX-EYE strip detector. Scans were taken on finely ground powders with a 0.02 step size, a 0.6 degree incident slit, and timeframes that varied from 1 to 8 h but were most frequently 2 h using 2 s per step. Measurements were taken at 30 kV and 10 mA. The specimens analyzed on this diffractometer included the CTL reference materials, NIST reference materials and purchased products.

At Edward C. Levy, specimens were prepared using a McCrone micronizing mill equipped with corundum grinding agents for 5 min. Internal standards of zinc oxide (CAS 1314-13-2) or α-silicon nitride (CAS 12033-89-5) were used at varying concentrations ranging from 8 to 50 wt% and incorporated using an agate mortar and pestle. Samples were prepared for analysis in a 2-mm sample indent sample holder. X-ray diffraction patterns were collected with a Rigaku MiniFlex 6G Benchtop X-ray diffractometer equipped with a Cu X-ray tube ($K\alpha_1 = 1.540593$, $K\alpha_2 = 1.54414$). Measurements were taken at 40 kV and 15 mA with an instrument radius of 150 mm, a step size of 0.01°, and from 3 to 90° 2Θ for 1–5 h. A 5° incident soller slit and a 1.25° divergence slit were used in a typical Bragg-Brentano geometry as incident optics. The receiving optics consisted of an 8 mm scattering slit, a 5° receiving soller slit, and a 0.3 mm receiving slit. The diffractometer was equipped with a Ni $K\beta$ filter to compensate for fluorescence interferences. A D/teX Ultra 0D/1D high-speed silicon strip detector was employed in the 1D, linear detector mode (12.8 mm × 20 mm active area, 10^6 cps/pixel count rate), with a variable knife edge to reduce scattering at lower angles.

At Pennsylvania State University, X-ray diffraction patterns were collected at 40 kV and 40 mA on a 240 mm radius Panalytical Empyrean® (third generation) θ-θ X-ray diffractometer equipped with a line source [Co $K\alpha_{1-2}$ (1.789010/1.792900 Å)] X-ray tube. Data were collected with a step size of 0.0167° from 10 to 85° 2θ. The incident optics consisted of a Bragg-Brentano HD® Co optic fitted with 0.04 rad. Soller slits, a 10-mm beam mask, 1/8° and 1/2° divergence, and anti-scatter slit, respectively. The diffracted optics included a PIXcel® detector with a 2.1223 active length in scanning line mode with a 1/4° programmable anti-scatter slit and 0.04 rad soller slits.

The authors noticed that the three diffractometers produced similar quality data with regards to signal to noise and peak width resolution. The authors conclude that for most cement phases the crystallite size was the dominant contribution to the peak width. At all three facilities, NIST SRM's are used to define the instrumental contributions under specific operating conditions. Furthermore, the authors believe that the data are representative from working diffractometers in the laboratory, for diffractometers that are not optimized for high resolution. However, it should also be noted that for most 1% concentration phases the peak areas were typically slightly above noise levels when using 1–2 h scans vs. longer data collection.

C. Quantitative phase analyses and data analyses

Three different whole pattern methods and two different types of analysis were used to determine the QPAs. The three methods were (1) whole pattern reference intensity ratio method (RIR), (2) Rietveld refinement, and (3) restricted parameter and block refined Rietveld refinement. The whole pattern RIR method (Fawcett *et al.*, 2015, 2019, 2020) is software embedded in the PDF-4 database product line. PDF-4+ Release 2022 was used for the analysis. The Rietveld analyses were performed using JADE-PRO (MDI, 2021) Table I provides a comparison of the three methods.

Initially, the authors explored the possibility of using totally automated QPA with both RIR and Rietveld methods.

TABLE I. Comparison of methods used in quantitative phase analysis

PDF-4+ RIR	Method Parameters	Rietveld JADE Pro	Modified Rietveld JADE Pro
Yes	Whole pattern modeling	Yes	Yes
Yes (peaks)	Intensities scaled and refined	Yes (profiles)	Yes (profiles)
	Refined Parameters		
No	Scale factor	Yes	Yes
No	Unit cell parameters	Yes	Yes
No	Temperature factor	Yes	Limits
No	Atomic positions	Yes	No
	User Options		
Yes (1D)	Orientation	Yes (multi)	Yes (multi)
Yes	Displacement	Yes	Yes
Yes	Transparency	Yes	Yes
Yes	Crystallite size-profile shape	Yes	No
Yes	Input amorphous profile	Yes	Yes
Yes	Set Internal standard	Yes	Yes
Yes	Can input material wo structure	Depends	Depends

https://doi.org/10.1017/S0885715622000215 Published online by Cambridge University Press

For various reasons described in the Results, totally automated methods produced unsatisfactory results. Based on the automated results and an analysis of the methods, including a review of prior published Rietveld refinements, a modified Rietveld method was developed with some parameter restraints and block refinement. In both the RIR and Rietveld methods, it was necessary to closely examine the pattern profile fitting and make adjustments when required, to obtain accurate results.

The QPA of all specimens using multiple methods were performed by the author, T. Fawcett. In the case of data sets from Edward C. Levy, there were complimentary XRF data as well as Rietveld analyses on all samples. The Rietveld analyses were performed by either Jessica Lyza at Edward C. Levy or Nichole Wonderling at Pennsylvania State University. These samples were mostly used to confirm additives and method development. Therefore, all the 22 samples from Edward C. Levy were analyzed by two people.

III. RESULTS

Phase identification confirmed the four major phases of Portland cement to be the calcium silicates C3S and C2S, and the calcium aluminates C3A and C4AF. Here, we are using cement chemist notation where the C stands for Ca expressed as CaO, the A for aluminum expressed as Al_2O_3 and F as iron expressed as Fe_2O_3. In this notation, C4AF is the chemical formula $Ca_4Al_2Fe_2O_{10}$ when expressed as oxides, but Ca_2AlFeO_5 is the structural formula. Furthermore, each of these cement chemist notations have polymorphs that are usually designated by their crystal systems. For example, C3S-M3 is the third known monoclinic structure of Ca_3SiO_5. Finally, three of the four major phases have more specific mineral name equivalents, hatrurite for C3S, beta-larnite for C2S, and brownmillerite for C4AF. The minerals names are more specific because there can be multiple minerals for some chemist notations. The frequent use of structurally non-specific cement chemist notation makes it difficult to reproduce many if not most published QPA results since the reader often does not know the exact structural reference used in the refinement. One of the purposes of this study was to try to identify exact structures which are noted by their unique Powder Diffraction File (PDF) number designations, each entry having a quality review and a cited reference publication. We will use cement chemist notation enabling comparison to other published works but also cite the specific PDF entry.

The Powder Diffraction File, PDF-4+ Release 2022, contains 1482 references that pertain to cement and cement hydration products. These are in a searchable subfile. In addition, there are >100 references that correspond to Ca_3SiO_5, Ca_2SiO_4, Ca_2AlFeO_5, and $Ca_3Al_2O_5$. A review of the publication dates for these references will show that many were not available when frequently developed methods, like ASTM C-1385, were first published, suggesting that the best references may not have been always used in QPA studies.

A. C3S, alite, hatrurite, and $Ca_3Si_2O_5$

The major phase of Portland cement, having desirable physical properties, is C3S. The exact polymorph of C3S is a matter of debate and different polymorphs have been cited in different publications. Here, we are helped by the large volume of cement publications that would indicate that the exact C3S polymorph in a specific cement, may depend on the nature and location of the minerals used in the clinker process and the trace cations in minerals that can dope into the Ca_3SiO_5–hatrurite structure in this high temperature process. Taylor in his book Cement Chemistry (Taylor, 1997) suggests that T2, M2, M3, and R polymorphs were found in cements from Australia. Courtial *et al.* (2003) identified that Mg doping seemed to stabilize M3 and that sulfates appeared to stabilize M1 polymorphs both of which were identified in cement plant samples. There have been two studies on NIST SRMs, one found the M3 polymorph (Pritula *et al.*) and another found a combination of R, T, and M3 (Peterson *et al.*, 2006). This later study used high resolution synchrotron and neutron data to examine the polymorphic mix. Very influential in the authors analysis are the studies of the C3S-M3 supercell structure (De la Torre and Aranda, 2002, 2003) and its influence on the accurate QPA of cements. The publication by Courtial *et al.* was also followed by private submission of key C3S polymorph data to the ICDD. The publication is important because it describes how you analyze for various monoclinic polymorphs using signature peaks and the data are important since they provide reference for those peaks.

When the authors studied both NIST and CTL references, commercial cements, and select clinker samples, the C3S-M3 polymorph was exclusively identified. As suggested (De la Torre and Aranda, 2002; Courtial *et al.*, 2003), these samples contained 1–3% MgO as determined by XRF or certificates of analysis.

The characteristic signatures of the M3 polymorph, such as the small triplet of peaks around 28°, from indexed supercell reflections, and the doublet at approximately 52° were found in all four known phase mixtures shown in Figure 1. Commercial samples typically have 8–12 phases which make the identification of the minor peak cluster at 28° more difficult, due to dilution and overlap from the additional phases. However, the strong peak at 52° rarely has any interferences and was used to confirm M3, as shown in Figure 2.

The ICDD database has four M3 supercell references, and three have crystal structures. The M3 polymorph is a disordered supercell with $Z = 36$. In one structure (PDF 04-009-5560), all calcium atoms are disordered at 50% occupancy, so there are 72 atom positions for calcium. In the other two structures (PDF 01-083-8362 and PDF 00-071-0563), half the Ca sites have unit occupancy and half are disordered, so there are 54 atom positions for Ca. The fourth reference is the submitted powder pattern by de Noirfontaine a coauthor in the Courtial publication, that matches very well to the calculated pattern from PDF 04-009-5560. If one examines the unit cell parameters and calculated densities of these four entries, they form a tight cluster within $Ca_3Si_2O_5$ with similar but not identical reduced cells, crystal cells, density, and molecular volumes. We speculate that these small differences may be due to small differences in Mg concentration and defect populations caused by the doping. In practice during search/match analyses of the various samples, the M3 polymorph was usually identified as the top statistical choice based on *d*-spacing analysis in both PDF-4+ and JADE-

https://doi.org/10.1017/S0885715622000215 Published online by Cambridge University Press

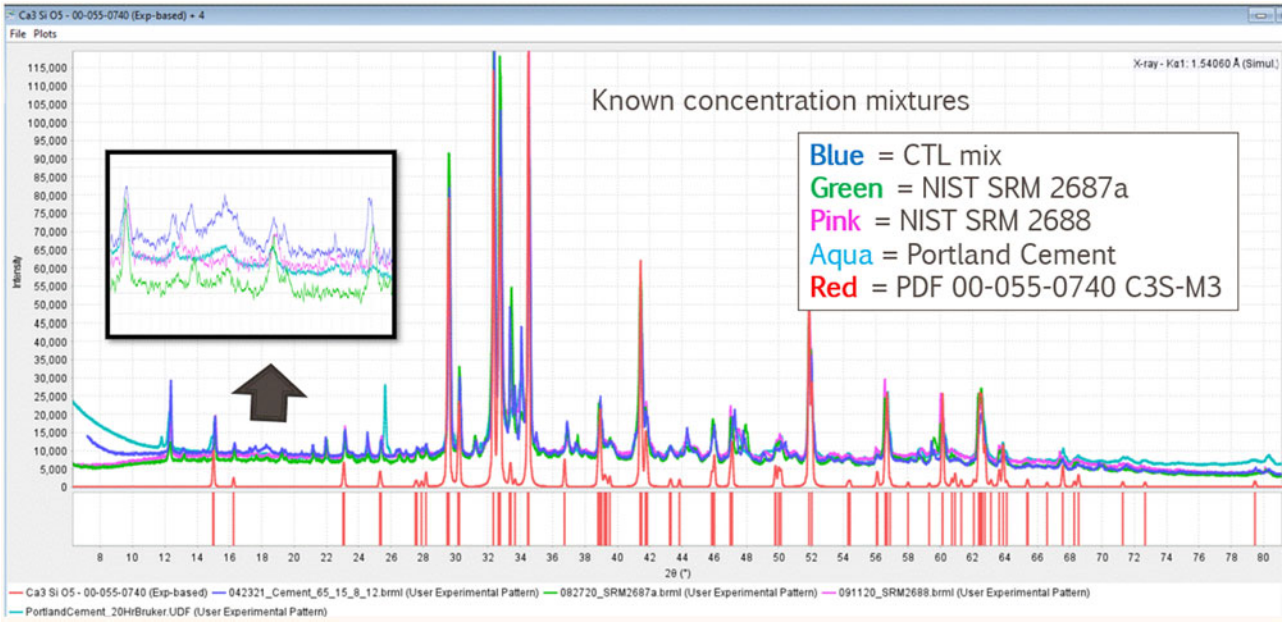

Figure 1. Known mixtures of phases, two certified SRMs from NIST, a CTL reference and a commercial cement. The commercial sample has additives in addition to the four major phases of Portland cement. Characteristic peak clusters for the M3 polymorph are shown in comparison with reference PDF 00-055-0740 and the arrows.

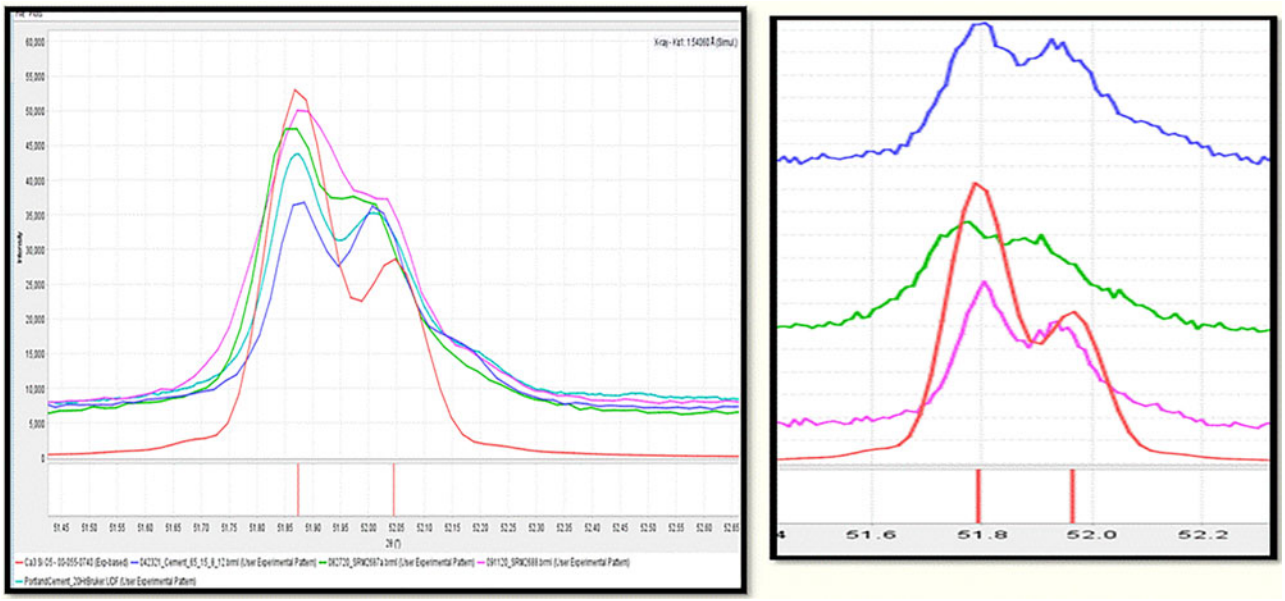

Figure 2. Characteristic C3S-M3 profile for PDF 00-055-0740, Window 5 described by Courtial *et al.* in 2003 in red at the bottom of both graphs. On the left, four known Portland cement mixtures are plotted and on the right are three commercial Portland cement mixes.

PRO. Occasionally, an M1 polymorph was the top choice and the R polymorph was sometimes seen in the top selections, however, the peak intensity profiles and characteristic clusters would always indicate the M3 polymorph.

The authors should note that all the samples analyzed originated in the United States. In the United States, many if not most, lime and calcite used in clinker processes have biogenic origin and low levels of Mg that would favor the M3 polymorph (Fawcett, 2021). Cements in other countries and from different kiln processes might favor other polymorphs as suggested in the literature.

At the beginning of the QPA study, the results from the phase identification process were directly fed into RIR and Rietveld analyses. It was quickly discovered that this often led to terrible results, especially if the wrong polymorph had been the top candidate in the search/match process. The above cited publications suggest that others had the same problem and if one examines the I/I_c values for different structures a huge variation is observed. This would be similar if scale factors from Rietveld analyses are examined. The selection of the inappropriate C3S polymorph directly leads to failure in the QPA. The best results are from references that reflect

https://doi.org/10.1017/S0885715622000215 Published online by Cambridge University Press

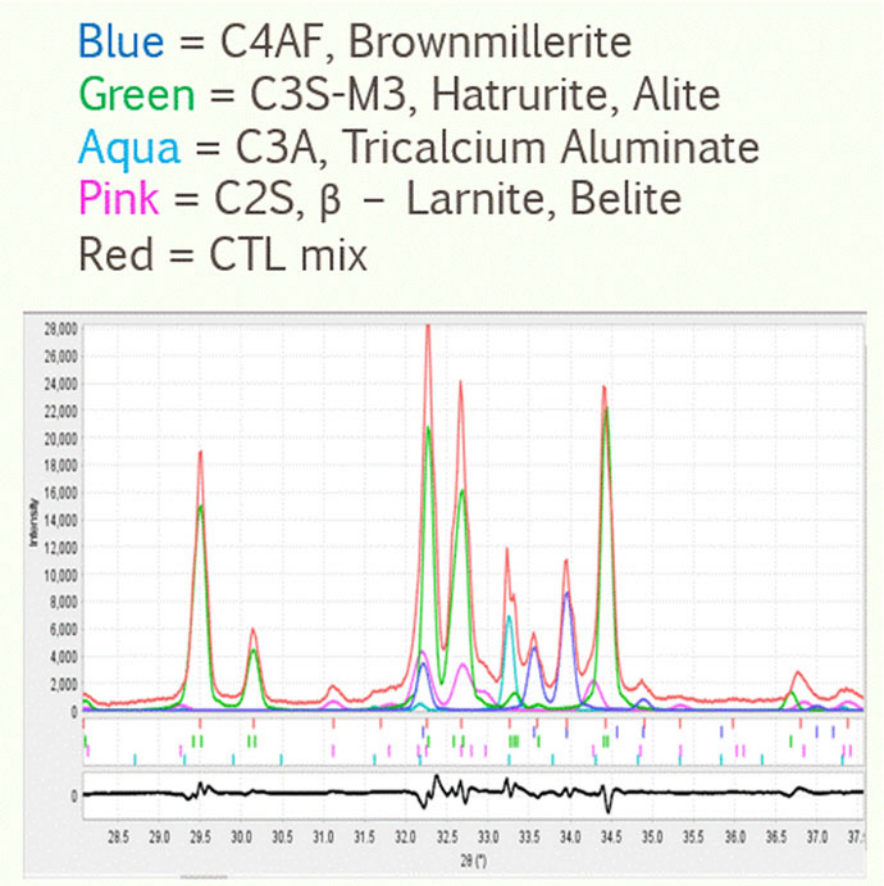

Figure 3. Selected area X-ray diffraction pattern of a Portland cement mix from CTL laboratories showing the four major phases that contribute to the observed peaks.

a doped disordered supercell produced from the clinker process as suggested by De la Torre and Aranda.

B. C2A, C3A, and C4AF

Any phase identification process, either graphically or through a careful analysis of *d*-spacings, will show that the typical Portland cement has a terrible peak overlap problem. For example, the largest peak in the pattern has intensity contributions from all four major phases (Figure 3). In the above CTL mix, we identified 95 observed peaks that had contributions from 230 reference intensities. In a commercial sample, with additives, we had 120 observed peaks that had over 350 contributions.

In order to determine the appropriate phases to use in the analysis, CTL references were used and compared with ICDD database. The CTL references were derived from high purity minerals and fired in an electric furnace. The minerals did have naturally occurring dopants. A separate QPA of these references found them to be >95% pure. The phase match was evaluated in two ways, first by a *d*-spacing comparison and goodness-of-merit and second by using a similarity index that examines intensities and profiles. Then, these selections were used in a custom data file set for search/match prior to QPA. If a reference scored in the top 4 of both statistical analytics it was considered for the control group, this resulted in 11 references for the major 4 phases a reduction of 90% of the possible choices. These 11 phases are shown in Table II.

It is interesting to note that the tricalcium aluminate, C3A, structures were also supercells. The supercells have extra peaks that are readily observed in cements, clinker, and reference samples. In references cited by the Highway Research Board, they referenced sodium-doped calcium aluminates but we found the above references to be statistically better, but the dopant is not specified. The brownmillerites identified have a Fe/Al ratio of 0.9–1.0. Variability in the ratio might be reasonable to expect from a clinker process and has been cited as a factor in QPA results from German sourced clinkers and Portland cement (Pritula *et al.*, 2003). The iron content has a dramatic influence on I/I_c values and scale factors calculated via Rietveld, so this would need to be looked at closely (both peak location and profile fitting) in any cement sample.

The CTL group routinely analyzes Portland cements from a variety of customer samples. They normally analyze for SiO_2, Al_2O_3, Fe_2O_3, CaO, MgO, SO_3, Na_2O, K_2O, TiO_2, P_2O_5, SrO, Mn_2O_3, ZnO, and Cr_2O_3 in all cements. Which accounts for most of the composition. The XRF results of 15 commercial Portland cements are summarized in Table III.

These six elements along with oxygen account for ~98% of the sample by weight, remaining oxides are all less than 1%. There is variability in the Al, Fe, S, and Mg concentrations as shown by the % root mean square. The data are consistent with variability in the C4AF phase concentration and the presence of the magnesium-doped C3S-M3 phase.

The CTL Group mentions that it would be unusual to find concentrations outside these ranges since cement producers need to carefully monitor composition and watch the liquid concentrations in the kiln to prevent kiln damage.

https://doi.org/10.1017/S0885715622000215 Published online by Cambridge University Press

TABLE II. Control group for major phases in Portland cement

Portland cement	Cement Notation		Z	PDF Number	Published	QM	Rank Similarity	Rank GOM
Ca_3SiO_5	C3S-M	M3	36	00-055-0740	2003	Star	3	3
Alite	C3S-M	*Supercell*	36	04-009-5560	1985	I	2	1
	C3S-M		36	00-071-0561	2011	Star	1	2
	C3S-M		36	01-083-8632	2002	Star	4	4
$Ca_3Al_2O_6$	C3A-C	Cubic	24	04-008-8069	1975	I	1	2
Tricalcium aluminate	C3A-C	*Supercell*	24	04-007-4797	1987	P	1	3
	C3A-O	Orthorhombic	12	00-033-0251	1979	Star	1	1
Ca_2SiO_4	C2S-beta	*Beta*	4	04-007-9746	1980	I	1	4
Larnite, Belite	C2S-beta		4	01-083-0460	1994	I	4	1
Ca_2FeAlO_5	C4AF		4	04-011-5939	2001	Star	1	1
Brownmillerite	C4AF	Al-rich	4	04-014-6640	2004	Star	4	2

The publication year is that of the reference, they were usually published in the PDF after review and editing. The similarity index and GOM ranking are in comparison with CTL references.

IV. METHOD

Once the control group of references was defined, the method was optimized by using the four samples with known concentrations. Analytics provided by PDF-4+ and JADE-PRO, as well as various display options, were primarily used to evaluate the quality of the profile fitting. Using JADE-PRO, the user has options for both automated and manual, RIR and Rietveld analyses. The authors did not use the RIR method in JADE-PRO. The selection of using the RIR method with PDF-4+ was based on evaluating recent improvements, described below, to the RIR software.

The RIR whole pattern fitting method produces semi-quantitative results when used in automatic modes. This is because unit cells and scale factors are not refined, and orientation and crystallite size adjustments currently require manual input. Since cement phases are frequently doped, small shifts were required to get the peak profiles to match perfectly. Indicator peaks, where the majority of the observed peak intensity was from a single phase, were used to evaluate scale and crystallite size. Fortunately, this information is provided in the search/match process which is intimately linked to the RIR module and the critical parameter adjustments can be made by toggles and sliders (recent additions). However, it must be mentioned that to get accurate results these adjustments were *always* required. Graphic options such as difference plots, summation, and offset plots, help the user make the required adjustments shown in Figure 4.

In Reitveld refinements, automatic refinements included unit cells, scale factors, temperature factors, and usually a 3-term peak profile for each phase. This refinement resulted in very low R factors and good analytics for nearly all data sets. However, a few data sets produced noisy difference plots and often gave a warning for correlated parameters (peak widths and temperature factors) and or unreasonable termperature factors. Visual examination would show that the C2S or C3A phase peak profiles were unrealistically broad. Not surprisingly these QPA results were poor despite the low R factors. Fortunately, similar results have been shown by other authors and these references also suggested solutions.

"In the majority of the refinements numerical instabilities were detected, leading to large correlations between FWHM and temperature parameters of some phases" (Pritula et al., 2003).

"The inclusion of additional phases into the Rietveld model increases the number of parameters being modeled, even when it is debatable that there is sufficient information in the data to identify the phases. This will result in a statistically better fit of the model, although the QPA results may be unrealistic" (Peterson et al., 2006).

Therefore, we went to a block refinement strategy, refining the scale and unit cell of C3S first since it is the major phase and has some strong indicator peaks. Then, the scale and unit cells of the other phases were added and refined. The refinement of the peak profiles and temperature factors were either put in restrictive limits or not refined. The profile widths were often determined with a separate analysis so that we would know reasonable limits when refining the mixtures. A similar block refinement strategy was used by Pritula, as well as Nicola *et al.* (2001) for online Rietveld analyses of cements.

Overall, this resulted in low R factors but often not as low as the automatic refinement, but the QPA results and peak profiles were much improved.

The final results are shown (Figure 5) for the 21 phases contained in the 4 known mixture samples of Portland cement. The absolute average error for the RIR-whole pattern method was 2.8% and the absolute average error for the block refined Rietveld method was 2.6%.

TABLE III. Mean and root-mean-square variations in 15 Portland cement samples

	Mean Concentration	RMS Concentration	% RMS
CaO	62.65	4.77	7.6
SiO_2	22.14	2.59	11.7
Al_2O_3	5.20	1.61	30.1
SO_3	2.90	0.88	30.4
Fe_2O_3	2.84	1.15	40.3
MgO	2.66	1.31	49.2
Sum	98.39		

A. Additives

A similar process is being used to characterize additives and reaction phases in cement products. The additives are typically not produced in the clinker process so we are not seeing the wide variability in defect structures and polymorph types. The references are usually being compiled by using search/

https://doi.org/10.1017/S0885715622000215 Published online by Cambridge University Press

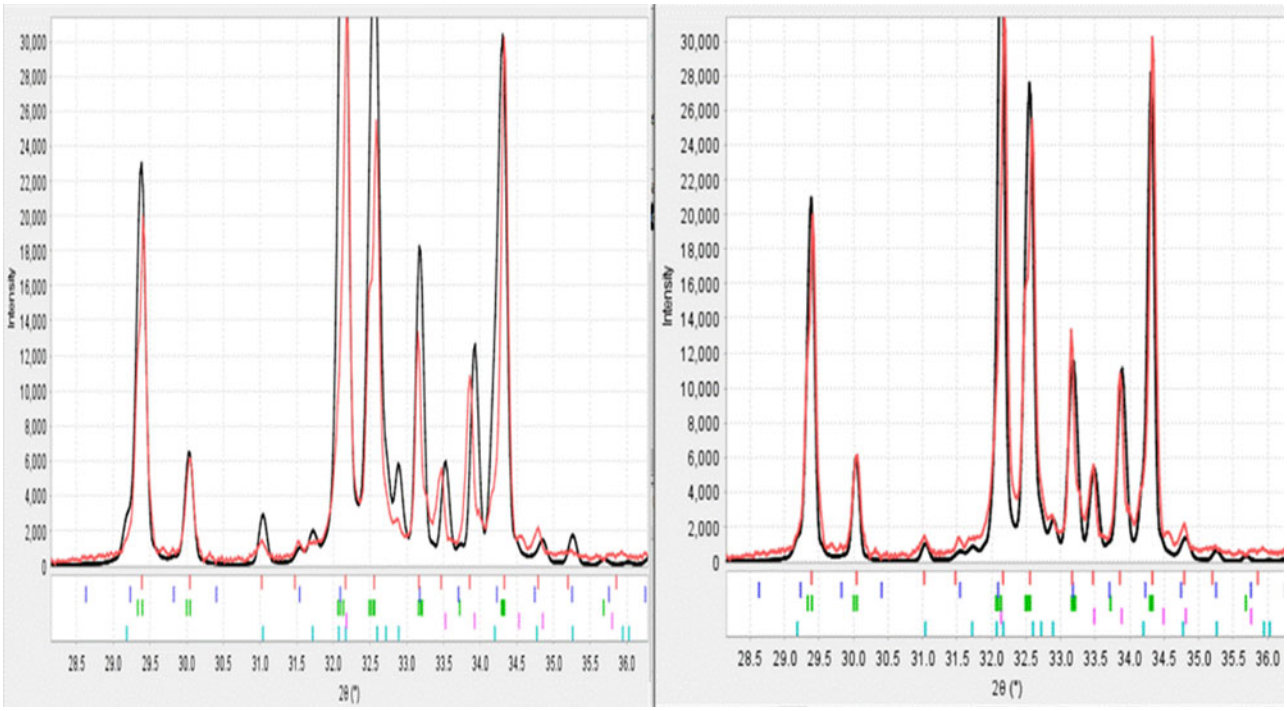

Figure 4. On the left, an automated whole pattern RIR least squares fit, on the right manual adjustment were made for peak shifts to the C4AF phase, and intensities of the C2S and C3S phases which are heavily overlapped. The experimental data are in red and the modeled four phase summation is shown in black.

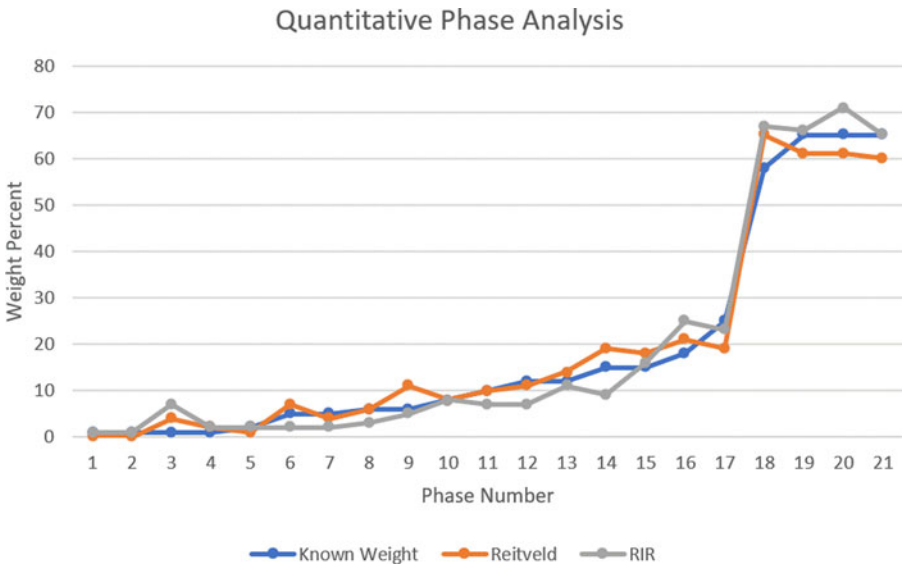

Figure 5. Comparison of QPA results vs. certified or known concentration of phases in Portland cement. Known values are plotted in blue and compared with modeled results using the RIR method (grey), and the Rietveld method (orange).

match techniques on commercial samples and ultimately need verification by QPA. This work is ongoing.

V. DISCUSSION

At the beginning of the study, we believed that the variability shown in prior Rietveld studies might be attributed to the lack of using standard databases and quality reviewed standard references. This is difficult to prove because the specific references are not cited in many publications and many authors input the structures themselves into the Rietveld refinement. We should also note that the PDF-4+ database was released in 2005 and many earlier studies did not use the C3S-MS supercells that were used as preferred models in later studies. This means that the availability of critical references often did not coincide with method development.

Overall, this review of cement references has proven beneficial since the review also included examination of subfile content, cement chemist notation, mineral designations, and cross references used in the PDF. The editor-in-chief and coauthor, Soorya Kabekkodu, has already edited several entries to reflect these updates for Release 2022.

Our experiences combined with literature review suggest that QPAs are not trivial due to significant overlapping peaks

https://doi.org/10.1017/S0885715622000215 Published online by Cambridge University Press

leading to correlated parameters in the refinements or difficulties with the overlap deconvolution in whole pattern RIR. In the latter case, the severe overlap between the C2S and C3S, especially in their respective concentration ranges, means that there are very few peaks of C2S that are sufficiently isolated to appropriately scale the phase. This means that the C3S phase is scaled and the C2S is scaled by difference. We and others have demonstrated that the selection of the appropriate polymorph is critical. We are also using models for describing a high-temperature kinetically fast clinker processes that may have a wide range of process and chemical variability. This variability may become wider in the future as companies try to produce environmentally friendly green cements. The three reference crystal structures of C3S-M3 are all slightly different. Is this process variability or limitations in the complex model of a disordered superstructure?

Can one do better? The answer is definitely yes! Lower detection limits and higher accuracy were demonstrated by Wallenta and Füllman (2004). They performed complimentary analytical studies to define the dopants in their cement plants, and then modified the structural models accordingly and did calibration studies. Nicola *et al.* (2001) used intensity profiles from plant cement samples to modify the C3S phase. Stutzman points out that a microabsorption correction may be required, particularly relative to C4AF and iron concentrations. High resolution and/or synchrotron studies can enable the detection of very weak peaks that help with refinement of supercell structures and occupancy factors and also help resolve the overlap issues – enabling better models and whole pattern fitting for QPA. They also may help with the detection of minor phases and/or detection of polymorphic mixes that may not be observable in a 1 or 2 h laboratory scan.

VI. CONCLUSION

A small collection of PDF references has been identified for the quantitative phase analysis of cements using laboratory diffractometers. These can be used as a control file for phase identification and QPA.

The C3S-M3 polymorph of Alite, a disordered supercell, was identified as the primary Portland cement phase in the cement samples examined, which were all produced in the United States. The authors found that the descriptive characterization by Courtial *et al.* (2003) was very useful in distinguishing between C3S monoclinic polymorphs.

Severe peak overlap was identified as the root cause of inaccurate results. In Rietveld whole pattern fitting, this manifested in refinement instabilities and correlated temperature factors and peak widths, where both could be refined to unrealistic values. In the RIR whole pattern method, this manifested in minor adjustments to peak width, position, and intensity scale to get the best results. A modified Rietveld block refinement with restrictions on peak widths and temperature factors was required to get the best result from laboratory data.

Conflict of interest

The authors have no conflicts of interest to declare.

American Standard Test Method C-1365-18, ASTM (**2018**). *Standard Test Method for Determination of the Proportion of Phases in Portland Cement and Portland Cement Clinker Using X-ray Powder Diffraction Analysis* (ASTM International, Conshohocken, PA, USA). The method was first issued in 1998 and last updated in March 2018.

Courtial, M., de Noirfontaine, M.-N., Dunstetter, F., Gasecki, G., and Signes-Frehel, M. (**2003**). "Polymorphism of tricalcium silicate in Portland cement: a fast visual identification of structure." Powd. Diff., **18**(1), 7–15.

De la Torre, A. G. and Aranda, M. A. G. (**2002**). "The superstructure of C3S from synchrotron and neutron powder diffraction and its role in quantitative phase analyses," Cem. Concr. Res. **32**(9), 1347–1356. doi:10.1016/S0008-8846(02)00796-2

De la Torre, A. G. and Aranda, M. A. G. (**2003**). "Accuracy in Rietveld quantitative phase analysis of Portland cements," Acta Crystallogr. Sect. B: Struct. Crystallogr. Cryst. Chem. **36**, 1169–1176. doi:10.1107/S002188980301375X

Fawcett, T. G. (**2021**). "Private Communication – over a period of several decades the author has studied many lime and calcite deposits by both XRD and XRF. In addition, he has studied Mg in calcite in a variety of shellfish, most notably quahogs, oysters and lightning whelks. Also see Berg, R. D., Solomon, E. A. and Tang, F.-Z. (2019). 'The role of marine sediment diagenesis in the modern oceanic magnesium cycle'," Nat. Commun., 1–10. doi:10.1038/s41467-019-12322-2

Fawcett, T. G., Kabekkodu, S. N., Blanton, J. R., Crowder, C. E., and Blanton, T. N. (**2015**). "Simulation tools and references for the analysis of nanomaterials," Adv. X-Ray Anal. **58**, 108–120. Simulation Tools and References for the Analysis of Nanomaterials (icdd.com).

Fawcett, T. G., Gates-Rector, S., Gindhart, A., Rost, M., Kabekkodu, S. N., Blanton, J. R., and Blanton, T. N. (**2019**). "Formulation analyses of high volume prescription drugs," Powder Diffr. **34**(2), 130–142. doi:10.1017/S0885715619000253

Fawcett, T. G., Gates-Rector, S., Gindhart, A. M., Rost, M., Kabekkodu, S. N., Blanton, J. R., and Blanton, T. N. (**2020**). "Total pattern analyses for non-crystalline materials," Powder Diffr. **35**(2), 82–88. doi:10.1017/S0885715620000263

Gates-Rector, S. D. and Blanton, T. N. (**2019**). "The Powder Diffraction File: a quality materials characterization database," Powder Diffr. **34**, 352–360.

Highway Research Board, HRB (**1972**). *Special Report 127, Guide to Compounds of Interest in Cement and Concrete Research* (Highway Research Board • Division of Engineering • National Research Council, National Academy of Sciences, National Academy of Engineering, Washington, DC).

MDI (**2021**). *JADE Pro (Computer Software)* (Materials Data, Livermore, CA, USA).

Nicola, V. Y. S., Madsen, I. C., Manias, C., and Retallack, D. (**2001**). "On-line X-ray diffraction for quantitative phase analysis: application in the Portland cement industry," Powder Diffr. **16**(2), 71–80. doi:10.1154/1.1359796

Peterson, V. K., Ray, A. S., and Hunter, B. A. (**2006**). "A comparative study of Rietveld phase analysis of cement clinker using neutron, laboratory X-ray and synchrotron data," Powder Diffr. **21**(1), 12–18. doi:10.1154/1.2040455

Pritula, O., Smrcok, L., and Baumgartner, B. (**2003**). "On reproducibility of Rietveld analysis of reference Portland cement clinkers," Powder Diffr. **18**(1), 16–22. doi:10.1154/1.1545116

Stutzman, P. and Heckert, A. (**2019**). *Certification of Standard Reference Material Clinker 2687a*; NIST Special Publication 260-195; U.S. Government Printing Office: Washington, DC. Available at: https://www.nist.gov/sites/default/files/documents/2019/05/14/sp260-195.pdf (accessed October 2019).

Stutzman, P., Lespinasse, G., and Leigh, S. (**2008**). *Compositional Analysis and Certification of NIST Reference Material Clinker 2686a*; NIST Technical Note 1602 (U.S. Government Printing Office, Washington, DC).

Taylor, H. F. W. (**1997**). *Cement Chemistry* (Telford, London).

Walenta, G. and Füllmann, T. (**2004**). "Advances in quantitative XRD analysis for clinker, cements, and cementitious additions," Powder Diffr. **19**, 40–44. doi:10.1154/1.1649328

Webster (2021). "Portland cement." *Merriam-Webster.com Dictionary*, Merriam-Webster. Available at: https://www.merriam-webster.com/dictionary/portland%20cement (accessed 14 August 2021).

https://doi.org/10.1017/S0885715622000215 Published online by Cambridge University Press